

ISSN 1561-8358 (Print)
ISSN 2524-244X (Online)

РАДИОЭЛЕКТРОНИКА, ПРИБОРОСТРОЕНИЕ
RADIOELECTRONICS, INSTRUMENT-MAKING

<https://doi.org/10.29235/1561-8358-2025-70-1-57-68>
UDC 620.179



Original article

Sviatlana O. Abetkovskaia^{1*}, Sergei A. Chizhik¹, Guangbin Yu²

¹*A. V. Luikov Heat and Mass Transfer Institute of the National Academy of Sciences of Belarus,
15, P. Brovka St., 220072, Minsk, Republic of Belarus*

²*School of Mechatronics Engineering, Harbin Institute of Technology,
92, Xida St., Nangang, 150001, Harbin, China*

**TAPPING MODE OF AN ATOMIC FORCE MICROSCOPE WITH A PROBE
CANTILEVER OF A LOW SPRING CONSTANT**

Abstract. The work presents mathematical simulation results of tapping interaction of an atomic force microscope (AFM) probe with low (0.1 N/m) spring constant of its cantilever with samples of materials with the Young moduli of 0.01; 0.1; 1; 10 GPa under varying the characterizing samples surface energy Hamaker constant, oscillation amplitude of a piezoelectric element, and also the quality factor of the probe. The Johnson–Kendall–Roberts model was used to describe contact between the probe and a sample. Non-contact interaction was taken into account using the Lennard–Jones potential. It was defined that at lower values of the Hamaker constant, higher quality factor of the AFM probe, and higher oscillation amplitude of the piezoelectric generator, conditions for transition from mixed mode of probe–sample interaction, which is undesirable for obtaining AFM images, to purely elastic mode occur. However, for materials with the Young moduli of 1 and 10 GPa abrupt changes in probe characteristics occur, which are associated not with influence of surface adhesion, but with late onset steady-state mode of probe oscillation. In order to avoid non-steady state oscillation of the probe in tapping AFM mode, it is proposed to use probes with higher spring constant to obtain high-quality AFM images of material surfaces with the Young modulus of 1 GPa and higher.

Keywords: atomic force microscopy, AFM, tapping mode, probe, probe spring constant, Young modulus, Hamaker constant

Acknowledgments: the work is performed within the framework of the project 3.03.3 of the State Program of Scientific Research “Convergence-2025” for 2021–2025 and the grant of Belarusian Republican Foundation for Fundamental Research no. T17KIG-009.

Conflict of interest: the team of authors includes the Editor-in-Chief of the Journal, Academician of the National Academy of Sciences of Belarus, Dr. Sci. (Engineering), Professor S. A. Chizhik.

Information about the authors: *Sviatlana O. Abetkovskaia* – Researcher at A. V. Luikov Heat and Mass Transfer Institute of the National Academy of Sciences of Belarus. <https://orcid.org/0009-0008-8806-0230>. E-mail: abetkovskaia@mail.ru; *Sergei A. Chizhik* – Academician of the National Academy of Sciences of Belarus, Dr. Sci. (Engineering), Professor, Head of the Department of Heat Transfer and Mechanics of Micro- and Nanoscale Systems at A. V. Luikov Heat and Mass Transfer Institute of the National Academy of Sciences of Belarus. <https://orcid.org/0000-0002-5301-0195>. E-mail: chizhik_sa@tut.by; *Guangbin Yu* – Dr. Sci. (Engineering), Professor, School of Mechatronics Engineering, Harbin Institute of Technology. E-mail: yugb@hit.edu.cn

Contribution of the authors: *Sviatlana O. Abetkovskaia* – search and analysis of literature data, setting up and conducting computational experiment, adjusting software, analyzing and interpreting results, formulating conclusions, writing and editing the manuscript; *Sergei A. Chizhik* – formulation a research problem, development research methodology, critical revision of the manuscript text, discussion the conclusions; *Guangbin Yu* – discussion the results and verification of their reproducibility.

For citation: Abetkovskaia S. O., Chizhik S. A., Guangbin Yu. Tapping mode of an atomic force microscope with a probe cantilever of a low spring constant. *Vesti Natsyyanal'nai akademii navuk Belarusi. Seryya fizika-tekhnichnykh navuk = Proceedings of the National Academy of Sciences of Belarus. Physical-technical series*, 2025, vol. 70, no. 1, pp. 57–68. <https://doi.org/10.29235/1561-8358-2025-70-1-57-68>

Received: 06.01.2025

Approved for publication: 06.03.2025

Signed to the press: 12.03.2025

Оригинальная статьяС. О. Абетковская^{1*}, С. А. Чижик¹, Гуанбин Ю²¹Институт тепло- и массообмена имени А. В. Лыкова Национальной академии наук Беларуси,
ул. П. Бровки, 15, 220072, Минск, Республика Беларусь²Факультет мехатроники, Харбинский технологический институт,
92, ул. Сиды, Наньган, 150001, Харбин, Китай**ПОЛУКОНТАКТНЫЙ РЕЖИМ АТОМНО-СИЛОВОГО МИКРОСКОПА
ПРИ МАЛОЙ ЖЕСТКОСТИ КОНСОЛИ ЗОНДА**

Аннотация. Методами математического моделирования исследовано полуконтактное взаимодействие зонда атомно-силового микроскопа (АСМ) малой (0,1 Н/м) жесткости его консоли с образцами материалов с модулем Юнга 0,01; 0,1; 1; 10 ГПа при варьировании постоянной Гамакера образца, характеризующей его поверхностную энергию, а также амплитуды колебаний пьезоэлемента и добротности зонда. Для описания контакта зонда и образца использовалась модель Джонсона–Кенделла–Робертса. Внеконтактное взаимодействие учтено с помощью потенциала Леннард–Джонса. Установлено, что при меньших значениях постоянной Гамакера, больших добротности АСМ-зонда и амплитуды колебаний пьезогенератора наступают условия перехода от нежелательного для получения АСМ-изображений смешанного режима взаимодействия зонда и образца к чисто упругому режиму. Однако для материалов с модулем Юнга 1 и 10 ГПа возникают скачкообразные изменения характеристик зонда, связанные не с влиянием поверхностной адгезии образца, а с поздним наступлением стационарного режима колебаний зонда. Во избежание неустойчивых колебаний зонда в полуконтактном режиме работы АСМ предложено использование более жестких зондов с целью получения высококачественных АСМ-изображений поверхностей материалов с модулем Юнга 1 ГПа и выше.

Ключевые слова: атомно-силовая микроскопия (АСМ), полуконтактный режим, жесткость консоли микрозонда, модуль Юнга, постоянная Гамакера

Благодарности: работа выполнена в рамках задания 3.03.3 Государственной программы научных исследований «Конвергенция–2025» на 2021–2025 годы и проекта Белорусского республиканского фонда фундаментальных исследований № Т17КІГ-009.

Конфликт интересов: в составе авторского коллектива – главный редактор журнала академик Национальной академии наук Беларуси, доктор технических наук, профессор С. А. Чижик.

Информация об авторах: Абетковская Светлана Олеговна – научный сотрудник Института тепло- и массообмена имени А. В. Лыкова Национальной академии наук Беларуси. <https://orcid.org/0009-0008-8806-0230>. E-mail: abetkovskaia@mail.ru; Чижик Сергей Антонович – академик Национальной академии наук Беларуси, доктор технических наук, профессор, заведующий отделением теплообмена и механики микро- и наноразмерных систем Института тепло- и массообмена имени А. В. Лыкова Национальной академии наук Беларуси. <https://orcid.org/0000-0002-5301-0195>. E-mail: chizhik_sa@tut.by; Гуанбин Ю – доктор технических наук, профессор, факультет мехатроники, Харбинский технологический институт. E-mail: yugb@hit.edu.cn

Вклад авторов: Абетковская Светлана Олеговна – поиск и анализ литературных данных, постановка и проведение вычислительного эксперимента, корректировка программного обеспечения, анализ и интерпретация результатов, формулирование выводов, написание и редактирование рукописи; Чижик Сергей Антонович – постановка задачи исследования, разработка методологии исследования, критический пересмотр текста рукописи, обсуждение выводов; Гуанбин Ю – обсуждение результатов и проверка их воспроизводимости.

Для цитирования: Абетковская, С. О. Полуконтактный режим атомно-силового микроскопа при малой жесткости консоли зонда (на англ. яз.) / С. О. Абетковская, С. А. Чижик, Гуанбин Ю // Весті Нацыянальнай акадэміі навук Беларусі. Серыя фізіка-тэхнічных навук. – 2025. – Т. 70, № 1. – С. 57–68. <https://doi.org/10.29235/1561-8358-2025-70-1-57-68>

Поступила в редакцию: 06.01.2025

Утверждена к публикации: 06.03.2025

Подписана в печать: 12.03.2025

Introduction. Tapping mode of atomic force microscopy is a widespread and fairly well-studied method for research material surfaces. In [1], a general solution of an equation for motion of a probe tip near a surface at amplitude and frequency modulations of an AFM was obtained, analytical expressions for average even force, average gradient of interaction force between a probe and a sample, and average damping constant during their interaction were given. However, behavior of a microprobe is so diverse when interacting with surfaces of various materials that, despite complex of knowledge about tapping mode, there remains a need to understand what kind of situation an AFM operator is dealing with. That allows choosing probe parameters and amplitude of the piezoelectric generator in order to obtain high-quality AFM images.

In the overwhelming majority of works, the Deryagin–Muller–Toporov (DMT) model is used for modeling tapping AFM mode [2–11]. Some studies consider viscoelastic probe–sample interaction in tapping mode of an AFM [8, 12–14]. In [15], simple analytical expressions were derived for direct calculation the reduced Hamaker constant, the Young modulus, the viscosity coefficient and relaxation time, but the solution is also based on the DMT model and doesn't take into account contact adhesion.

In this investigation, not only non-contact attractive probe–sample interaction is taken into account, but also contact adhesion using the Johnson–Kendall–Roberts model for contact of a sphere and a plane [16], which is more accurate approximation to their real interaction than the DMT model. It is especially important to take into account the non-contact and contact attractions of a probe and a sample when studying conditions for onset mixed mode of probe operating. In mixed (transient) mode, spontaneous switching between the modes of attractive and repulsive interaction with a sample occurs, due to which defects appears in the AFM images of material surfaces, so it should be avoided. When performing such study using mathematical modeling methods, we revealed a situation that does not fit into a general scheme. In this regard, there was a need for separate study interaction of the microprobe cantilever, which has a low spring constant, with materials characterized by different values of the Young modulus and the surface energy, and this is the subject of this work. Typically, probes with cantilevers as low as 0.1 N/m are intended for contact AFM mode, but some manufacturers offer to use its in tapping mode.

Mathematical model. An equation of probe oscillation in tapping (intermittent-contact) mode of interaction with a sample was solved using mathematical simulation methods. Model (1), which has been tested many times previously and is in good agreement with experimental data [17], was taken as base. An expression for probe–sample interaction $F_{ts}(z)$ takes into account both non-contact attractive interaction according to Lennard–Jones and elastic-adhesive probe–sample contact. The latter occurs in the lower part of a probe oscillation cycle and is described using the Johnson–Kendall–Roberts model.

The equation of probe tip oscillation is

$$mz'' + \frac{m\omega_0}{Q}z' + k(z - z_{\text{pos}}) = a_{\text{bm}}k\sin(\omega t) + F_{ts}(z), \quad (1)$$

where m is mass of the microprobe, kg; z'' is the second derivative of vertical displacement of the tip probe, nm/s²; ω_0 is the natural angular frequency of the probe, Hz; z' is derivative of vertical displacement of the tip probe, nm/s; Q is the quality factor of the cantilever; k is the spring constant of the probe cantilever, N/m; z is vertical displacement of the tip probe, nm; z_{pos} is a position of a cantilever fixing point above a sample surface, nm; a_{bm} is the oscillation amplitude of the piezoelement, on which the cantilever is fixed, nm; ω is operating angular frequency of the probe, Hz; t is time, s; F_{ts} is the interaction force between the probe and a sample surface, nN. Here the force of probe–sample interaction is

$$F_{ts}(z) = \begin{cases} F_{\text{LJ}}(z), z > z_{F_0} \\ F_{\text{JKR}}(z), z \leq z_{F_0} \end{cases}, F_{\text{LJ}}(z) = -\frac{HR}{6} \left(\frac{1}{z^2} - \frac{\sigma^6}{4z^8} \right), F_{\text{JKR}} \left(\frac{z}{z_c} \right) = \left(\frac{z}{z_c} \left(\frac{F_{\text{JKR}}}{P_c} \right) \right)^{-1},$$

$$\frac{z}{z_c} = \begin{cases} -\left(3\sqrt{\frac{F_{\text{JKR}}}{P_c} + 1} - 1 \right) \left[\frac{1}{9} \left(\sqrt{\frac{F_{\text{JKR}}}{P_c} + 1} + 1 \right) \right]^{1/3}, & \frac{z}{z_c} \leq 3^{-2/3}, \\ \left(3\sqrt{\frac{F_{\text{JKR}}}{P_c} + 1} + 1 \right) \left[\frac{1}{9} \left(1 - \sqrt{\frac{F_{\text{JKR}}}{P_c} + 1} \right) \right]^{1/3}, & 3^{-2/3} \leq \frac{z}{z_c} \leq 1, \end{cases}, z_c = \frac{1}{3R} \left(\frac{3RP_c}{k_s} \right)^{2/3}, P_c = \frac{3}{2} \pi R \Delta\gamma,$$

$$\Delta\gamma = \frac{H}{16\pi\sigma^2}, k_s = \frac{4}{3\pi} \cdot \frac{1}{\kappa_1 + \kappa_2}; \kappa_i = \frac{1 - \nu_i^2}{\pi E_i}, i = \overline{1, 2}.$$

Here F_{LJ} is the non-contact interaction force, nN; F_{JKR} is the contact interaction force according to the Johnson–Kendall–Roberts model, nN; z_{F_0} is a distance, at which the contact and non-contact interaction forces are balanced, nm; H is the Hamaker constant of a sample, aJ; R is radius of probe tip curvature, nm;

σ is the interatomic distance, nm; P_c is the maximum force of adhesion, nN; $\Delta\gamma$ is specific surface energy of a sample, J/m^2 ; k_s is a reduced modulus of elasticity of sample and tip materials, GPa; ν_1, ν_2 are the Poisson's ratios of tip and sample materials, respectively; E_1, E_2 are the Young modulus of tip and sample materials, respectively, GPa; $aJ = 10^{-18} J$ – attojoule.

Initial conditions are: $z(0) = z_{\text{pos}}, z'(0) = 0$.

In order to reproduce a situation of the probe–sample interaction during AFM scanning, mathematical simulation was performed for distances z_{pos} between the attachment point of the cantilever and a sample from zero to values close to values of free oscillation amplitude of the probe tip. It is necessary to vary the distance z_{pos} during simulation, since it changes during scanning. Height of the tip was neglected.

As a result of the simulation, sets of dependences of the amplitude, phase shift of probe tip oscillation, depth of deformation of a sample by the probe, the probe–sample interaction force at the bottom point of a tip oscillation cycle (at the maximum penetration of the probe into a sample) on the distance z_{pos} were obtained. Herewith, following parameters were varied: the Young modulus of sample material (from 0.01 to 10 GPa); the Hamaker constant characterizing surface energy of a sample (from 0.1 to 0.3 aJ); the oscillation amplitude of the piezoelectric element forcing vibration of the microcantilever (from 0.5 to 2 nm); the quality factor of the probe cantilever (from 20 to 200). The quality factor was changed because in practice, when an operator chooses the probe, its Q -factor is unknown in advance. It can be determined using amplitude-frequency characteristics of the probe. The microcantilever with a spring constant of 0.1 N/m was investigated. Radius of curvature of the probe tip was set equal to 10 nm, the Young modulus of probe material was 179 GPa (corresponds to silicon), and the natural frequency of probe oscillation was 38.9 kHz. Oscillation was excited at resonance.

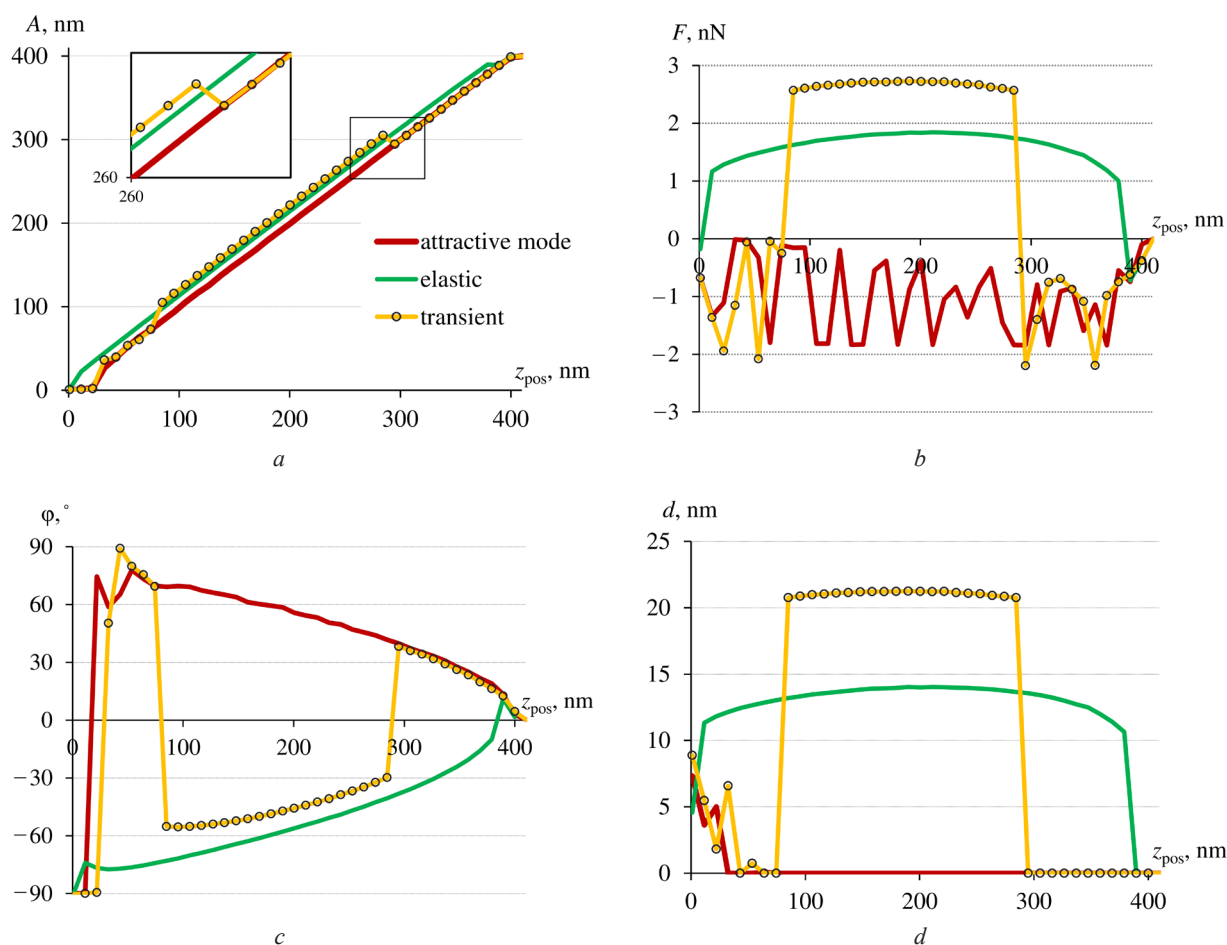


Figure 1. Characteristics of the elastic, attractive and mixed modes of probe–sample interaction: a – the oscillation amplitude of probe tip vibration; b – the probe–sample interaction force at the bottom point of its oscillation cycle; c – phase shift of tip oscillation; d – the maximum deformation depth of the sample by the probe

The obtained dependences were analyzed for presence of switches between the repulsive and attractive modes of probe–sample interaction. Interaction mode was recognized as purely elastic (repulsive) for a certain set of input parameters (E, H, a_{bm}, Q) if a curve of the probe oscillation amplitude versus the distance z_{pos} was monotonic over an entire interval $0.05 \leq A/A_0 \leq 0.95$ and the probe–sample interaction force at the bottom point of a probe oscillation cycle was positive (Figure 1).

Here, A_0 and A are the amplitude of probe free oscillation and its operating amplitude, respectively. Attractive mode of probe–sample interaction was recognized as mode in which the probe oscillation amplitude curve was monotonic and the probe–sample interaction force was negative over the same interval of a relative amplitude of probe oscillation. All other cases are attributed to mixed (transient) interaction mode, when switching occurs between the modes of attraction and repulsion of the probe and a sample, accompanied by abrupt changes in the dependence of the probe oscillation amplitude on the distance z_{pos} .

Data representation structure. The results of simulation of the probe–sample interaction modes are presented in form of diagrams (Figure 2). In them the values of the Young modulus and the Hamaker constant are marked on the X and Y axes respectively, for which the simulation was performed. Circles, triangles, and crosses indicate, respectively, the elastic, attractive, and mixed modes of probe–sample interaction, realized with certain combinations of simulation input parameters indicated in the diagrams. Each point in the diagram corresponds to a set of four curves: the dependences of the amplitude, phase shift of probe oscillation, the maximum deformation depth of a sample by the probe, and the probe–sample interaction force at the lower point of a probe oscillation cycle on the z_{pos} distance, similar to those shown in Figure 1.

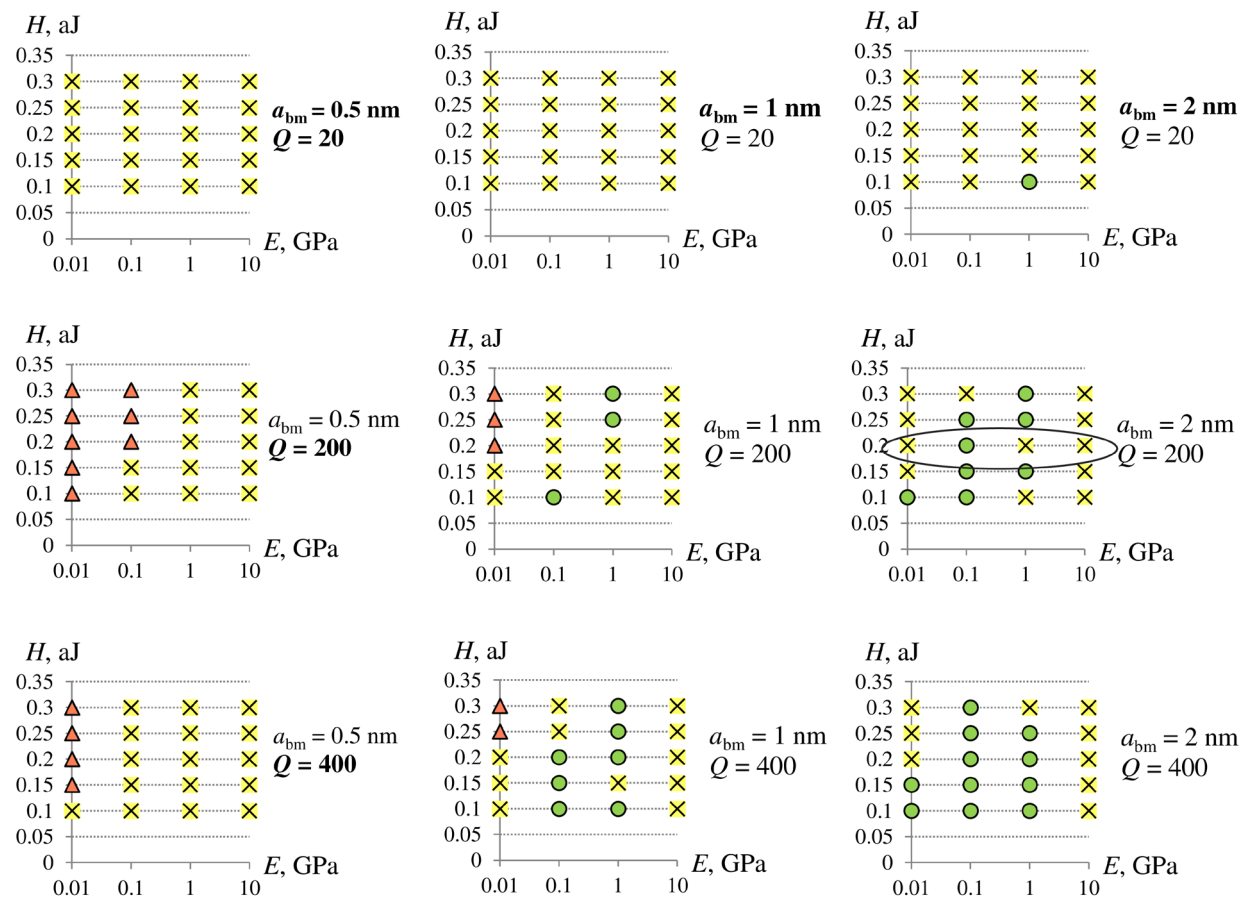


Figure 2. Diagrams of the interaction modes of the probe with a spring constant of 0.1 N/m with samples, realized at different values of the Young modulus and the Hamaker constant of samples, the oscillation amplitude of the piezoelectric generator and the probe quality factor:
 ▲ – attractive interaction mode; ● – elastic mode; ✕ – transient mode

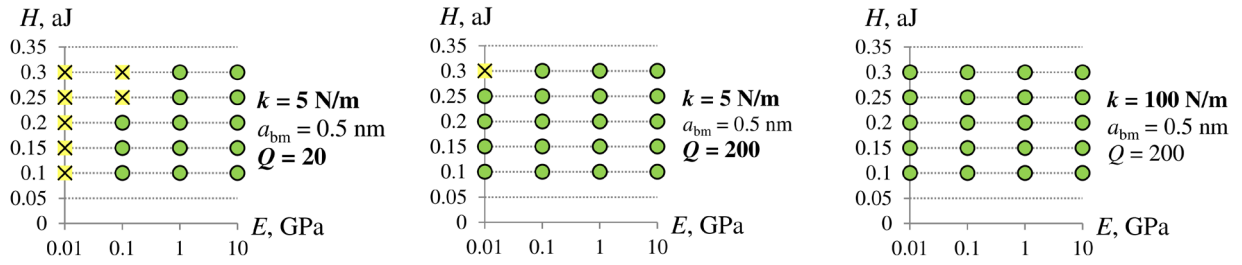


Figure 3. Diagrams of the interaction modes of probes with a spring constant of 5 and 100 N/m with samples, realized at different values of the Young modulus and the Hamaker constant of samples, the oscillation amplitude of the piezoelectric generator of 0.5 nm and the probe quality factors of 20 and 200:
● – elastic interaction mode; ✕ – transient mode

Results and discussion. For materials with the Young modulus of 0.01 and 0.1 GPa, a following regularity is observed. Increase in the oscillation amplitude of the piezoelectric element and the probe quality factor, as well as lower values of the Hamaker constant lead to transition from the mixed mode of probe–sample interaction to the elastic mode. However, for the Young modulus of sample material of 10 GPa, only the mixed mode of interaction is realized. For the sample Young modulus of 1 GPa, the mixed and elastic modes appear chaotically and unsystematically in the diagrams. This fact requires explanation, especially since calculations performed for higher cantilever spring constants (5 and 100 N/m) fit into the pattern of achieving the purely elastic mode of probe–sample interaction by increasing a_{bm} , Q and decreasing H for the samples Young modulus of 0.01; 0.1; 1; 10 GPa. Examples of the diagrams for a spring constant of 5 and 100 N/m are shown in Figure 3.

In order to study this fact, we will consider curves of the probe–sample interaction force at the bottom point of a probe oscillation cycle (Figure 4). We take $a_{\text{bm}} = 2 \text{ nm}$, $Q = 200$, and vary the Young modulus and the Hamaker constant of a sample. For the Young modulus of a sample of 0.1 GPa, the dependence of the force on z_{pos} undergoes a jump twice: from attraction (negative force values) to repulsion (positive values) and vice versa (see Figure 4, *a*). In this case, for the Hamaker constant values of 0.10–0.25 aJ, the jumps on the force curves are located outside the interval $0.05 \leq A/A_0 \leq 0.95$, therefore these curves are attributed to the elastic interaction mode. The force curve at $H = 0.3 \text{ aJ}$ has jumps shifted inside the significant interval, therefore it is attributed to the transient interaction mode.

At the Young modulus of 1 GPa, in addition to one switching outside the considered interval of the relative amplitude of probe oscillation (in a region of z_{pos} near 400 nm), several force curves also have chaotic switchings in a z_{pos} interval from 0 to 30 nm (see Figure 4, *c*). Such switchings become even more numerous at the sample Young modulus of 10 GPa, and the interval in which they are observed expands to 85 nm (see Figure 4, *e*).

As shown by dependences of the interaction force on a coordinate of the tip at the bottom point of its oscillation cycle Z_{min} , at $E = 0.1 \text{ GPa}$ the tip probe deforms sample material by the maximum of 5 nm, and force values are up to 4 nN (see Figure 4, *b*). At $E = 1 \text{ GPa}$ the maximum probe deepening is only 2 nm, and the elastic force already reaches 14 nN (see Figure 4, *d*). At $E = 10 \text{ GPa}$ the deformation depth of the samples is less than 1 nm, i.e. they are practically not deformed, while the elastic reaction force of the samples increases to 36 nN (see Figure 4, *f*). Thus, with increase in the Young modulus of sample material, its semi-contact interaction with the probe becomes increasingly rigid.

Further, we fix the Hamaker constant ($H = 0.2 \text{ aJ}$) and consider energy losses of the probe per oscillation cycle (power dissipation) during interaction with materials of different Young modulus (Figure 5). Power dissipation of the probe were calculated using a formula

$$P_{\text{tip}} = \frac{kA\pi\omega_0}{Q}(A_0 \cos\varphi - A),$$

proposed in [18], with a difference that the sine was replaced by the cosine, since in our case a driving force was specified as $a_{\text{bm}}k\sin(\omega t)$ (see (1)). The calculation was performed for $a_{\text{bm}} = 2 \text{ nm}$, $Q = 200$, E from 0.01 to 10 GPa (indicated by an ellipse in the interaction mode diagram in Figure 2).

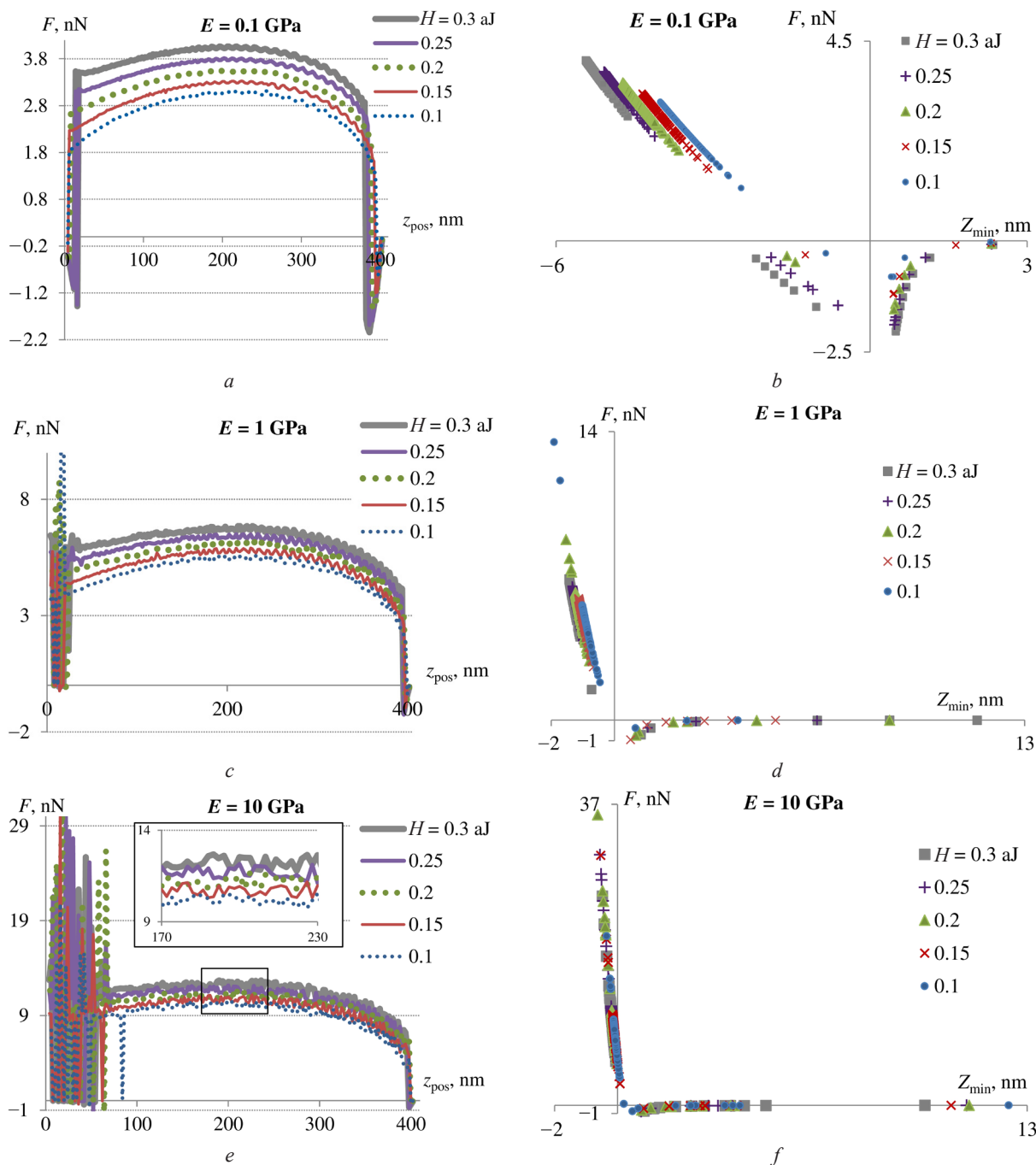


Figure 4. Dependences of the interaction force of the probe with material samples: *a, c, e* – on the distance z_{pos} ; *b, d, f* – on the position Z_{min} of the probe tip at the bottom point of its oscillation cycle

Curves of a dependence of the energy losses by the probe show a fundamental difference in interaction processes of the probe with a spring constant of 0.1 N/m with low-modulus and higher-modulus samples. Power dissipated by the probe during interaction with materials of the Young modulus of 0.1 and 0.01 GPa are about 0.25 and 2.4 pW, respectively. During interaction with samples of the Young modulus of 1 and 10 GPa, no energy losses by the probe occur, except for some points on the curves at small values of the z_{pos} distance, corresponding to points of chaotic behavior on curves of the probe–sample interaction force (Figure 5, *b*). For comparison, dependences of the probe–sample interaction forces and the energy losses by the probe for purely elastic semi-contact interaction of the probe and a sample were calculated according to the Hertz model. These curves of the energy losses by the probe also demonstrate absence of the energy losses by the probe (due to a fact that elastic forces are conservative) and sharp energy drops at some points z_{pos} for samples with the Young

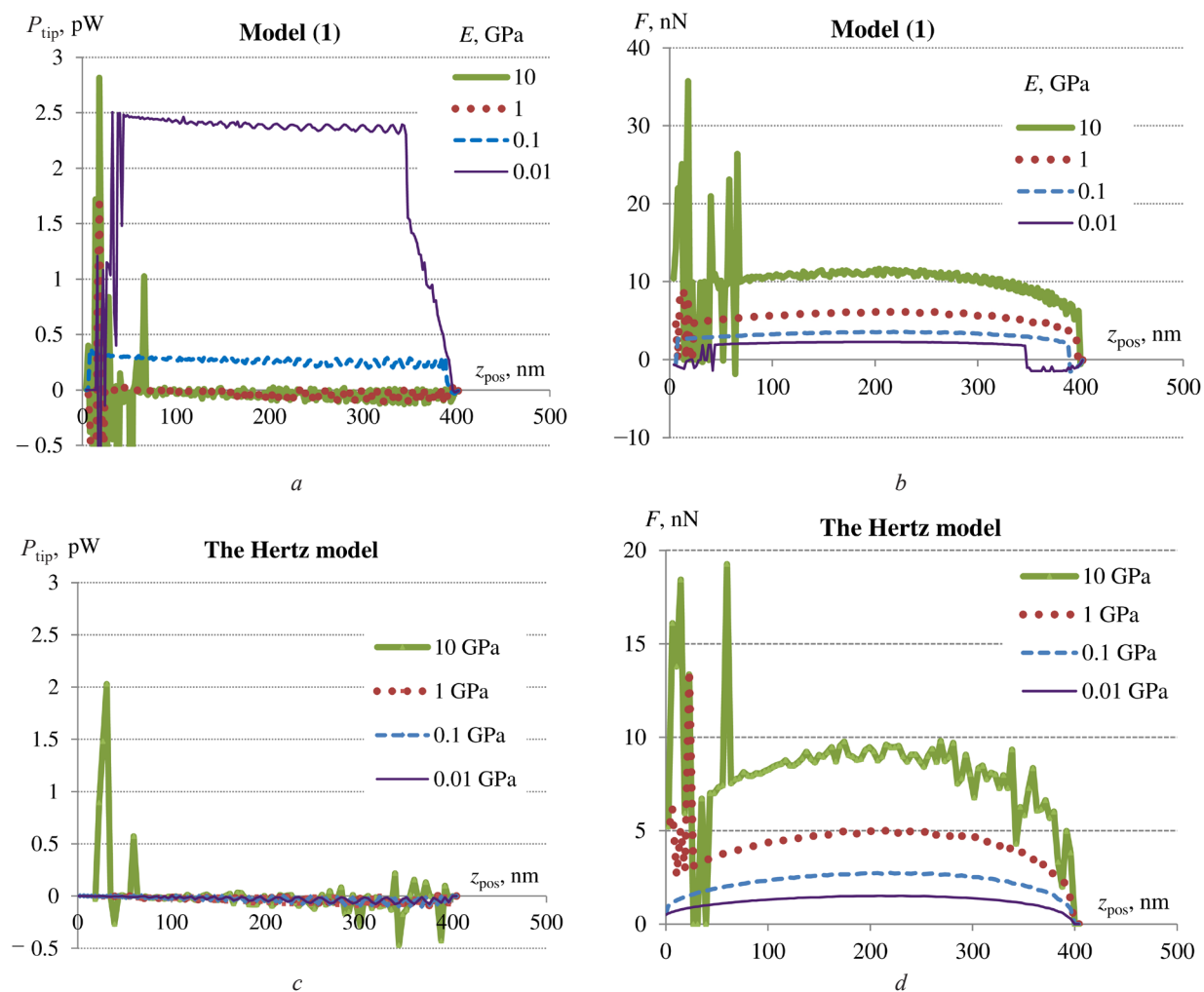


Figure 5. Dependences of characteristics of probe–sample interaction on the distance z_{pos} , calculated using model (1) (*a*, *b*) and using the Hertz model (*c*, *d*): *a*, *c* – the energy losses by the probe per oscillation cycle; *b*, *d* – the interaction forces

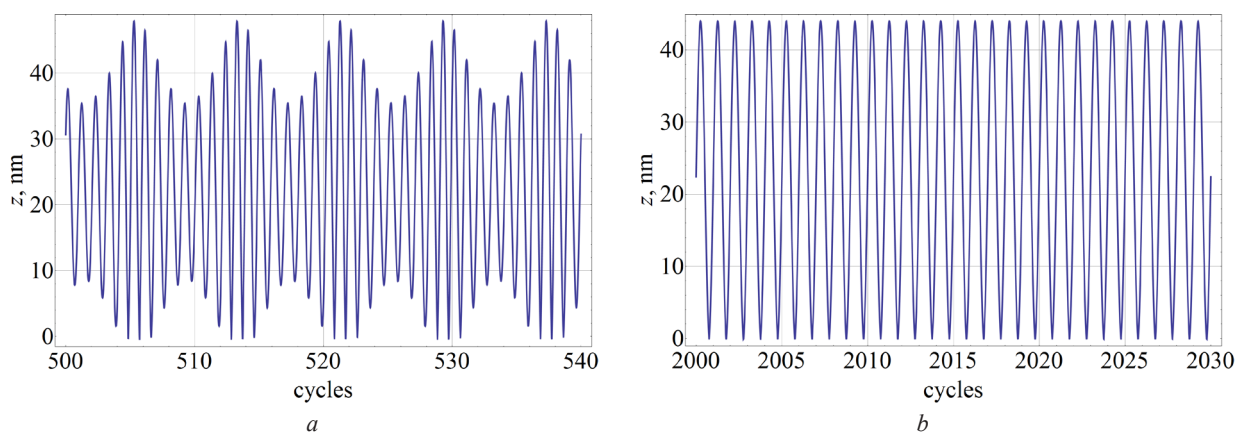


Figure 6. Motion of the probe tip during interaction with a sample surface, characterized by the Young modulus of 10 GPa and the Hamaker constant of 0.2 aJ, with the oscillation amplitude of the piezoelectric element of 2 nm, the probe quality factor of 200, and the distance between the probe attachment point and sample $z_{\text{pos}} = 22$ nm:
a – the non-steady-state mode of tip oscillation (the graph is shown starting with $2.5Q$ oscillation cycles);
b – the steady-state mode (starting with $10Q$ oscillation cycles)

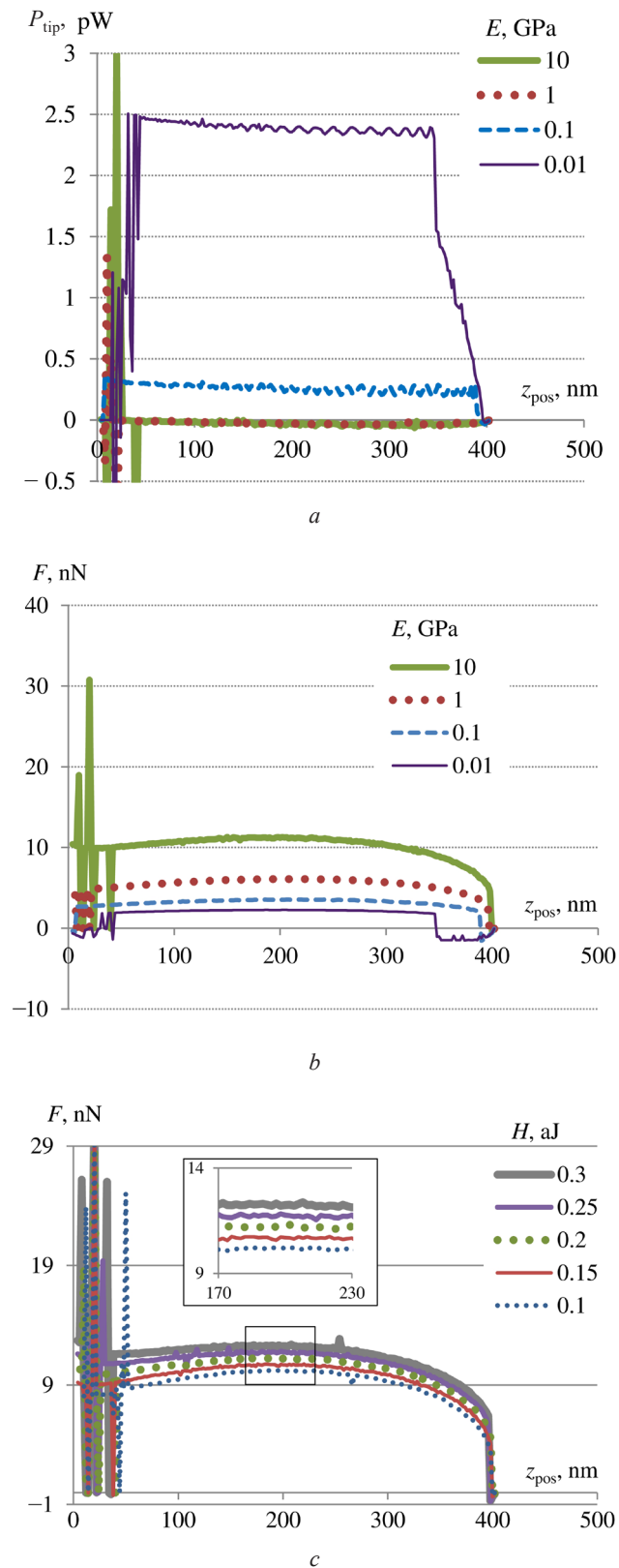


Figure 7. Dependences of the characteristics of probe–sample interaction on the distance z_{pos} after $20Q$ cycles of probe oscillation ($a_{\text{bm}} = 2$ nm, $Q = 200$):
 a – the energy losses by the probe per oscillation cycle ($H = 0.2$ aJ); b – the interaction forces ($H = 0.2$ aJ);
 c – the interaction forces ($E = 10$ GPa)

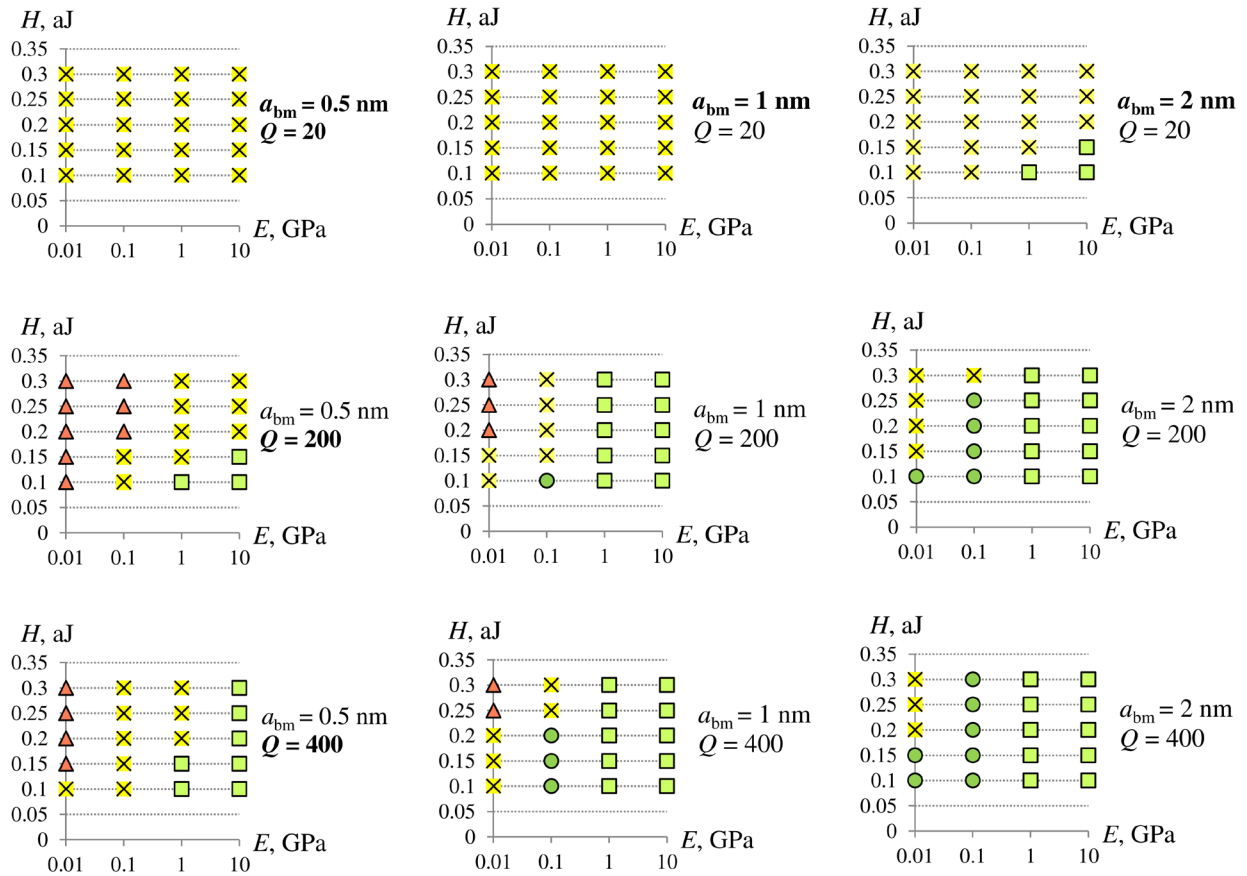


Figure 8. Diagrams of the interaction modes of the probe with a spring constant of 0.1 N/m with samples, realized at different values of the Young modulus and the Hamaker constant of samples, the oscillation amplitude of the piezoelectric generator and the probe quality factor: \blacktriangle – attractive interaction mode; \bullet – elastic mode; \times – transient mode; \blacksquare – conditionally elastic mode

modulus of 1 and 10 GPa (Figure 5, *c*), which are also presented in the force curves (Figure 5, *d*). Consequently, the sharp switches in the force curves, and hence the amplitude of probe oscillation and its phase shift, occurring during interaction of the probe with a spring constant of 0.1 N/m with samples of the Young modulus of 1 and 10 GPa, are no way related to surface adhesion of the samples for interaction model (1) too.

A reason for such chaotic behavior of the probe during interacting with materials of the Young modulus of 1 and 10 GPa is instability of the probe oscillation mode (Figure 6, *a*). Usually, the steady-state mode is achieved after $2Q$ cycles of probe oscillation, but when a soft probe interacts with such material samples, the steady-state mode at some distances z_{pos} occurs much later (Figure 6, *b*), and in some cases, as modeling shows, does not occur even after $50Q$ oscillation cycles. Figure 7 shows curves of the probe–sample interaction forces and the probe energy losses, modeled after $20Q$ cycles of probe oscillation (compare Figures 7, *a, b* with Figures 5, *a, b*; Figure 7, *c* with Figure 4, *e*).

Thus, it is possible to reduce a number of the switches between the attractive and repulsive modes by increasing probe oscillation time at each point over a sample surface (Figure 7). However, this is not always feasible in practice, since it will increase scanning time several times/tens of times. Therefore, it is better to choose probes with higher spring constant for samples with the Young modulus of 1 and 10 GPa. Another recommendation can be to use not too high values of the feedback parameter *set-point*. For a sample of 1 GPa, this will avoid the z_{pos} distances at which the attractive/repulsive modes are switched.

Appearance of the jumps on the curves of the interaction force and the energy losses during interaction of the probe with a sample of the Young modulus of 0.01 GPa (see Figures 5, *a, b* and 6, *a, b*) is associated with confrontation of the repulsive and attractive forces, since similar curves constructed

using the Hertz model for this sample do not have jumps (see Figures 5, *c*, *d*). Although it should be noted that in this case there is also the non-steady-state mode of probe oscillations at some distances z_{pos} .

Thus, taking into account specificity of the chaotic jumps, which appeared on the curves of the interaction characteristics of the probe with a spring constant of 0.1 N/m with materials of the Young modulus of 1 and 10 GPa, which are not associated with surface adhesion of samples, the interaction mode can be conditionally classified as purely elastic (Figure 8). However, corresponding sets of the input parameters of such probe–sample interaction are not suitable for AFM scanning.

Conclusion. The article studies dynamic semi-contact interaction of the probe of low spring constant (0.1 N/m) with material samples having the Young modulus of 0.01; 0.1; 1; 10 GPa, the Hamaker constant of 0.1–0.3 aJ at piezoelectric element oscillation amplitudes of 0.5; 1; 2 nm and the probe quality factor of 20, 200, 400. It is found that increase in the oscillation amplitude of the piezoelectric generator, higher values of the probe quality factor and, as well as lower values of the Hamaker constant, allow switching from the transient mode of probe–sample interaction, which occurs due to confrontation between elastic repulsion and adhesive attraction of the probe and a sample and is unsuitable for obtaining high-quality AFM images of materials, to the purely elastic interaction mode. However, for samples with the Young modulus of 1 and 10 GPa, the abrupt changes in the interaction characteristics occur that are in no way related to surface adhesion of a sample, but only with onset of the steady-state probe vibration mode much later than after $2Q$ cycles of its oscillations. In practice, this means that obtaining high-quality AFM images with a low-rigidity probe can be achieved by repeatedly reducing a scanning speed, which is not always acceptable. Therefore, it is possible to recommend using probe cantilevers that are more rigid than 0.1 N/m for materials of the Young modulus of 1 GPa and higher.

References

1. Songen H., Bechstein R., Kuhnle A. Quantitative atomic force microscopy. *Journal of Physics: Condensed Matter*, 2017, vol. 29, no. 27, pp. 274001–1–17. <https://doi.org/10.1088/1361-648X/aa6f8b>
2. Garcia R., San Paulo A. Attractive and repulsive tip-sample interaction regimes in tapping-mode atomic force microscopy. *Physical Review B*, 1999, vol. 60, no. 7, pp. 4961–4967. <https://doi.org/10.1103/PhysRevB.60.4961>
3. Stark M., Stark R. W., Heckl W. M., Guckenberger R. Inverting dynamic force microscopy: From signals to time-resolved interaction forces. *The Proceedings of the National Academy of Sciences (PNAS)*, 2002, vol. 99, no. 13, pp. 8473–8478. <https://doi.org/10.1073/pnas.122040599>
4. Lee S. I., Howell S. W., Raman A., Reifengerger R. Nonlinear dynamics of microcantilevers in tapping mode atomic force microscopy: A comparison between theory and experiment. *Physical Review B*, 2002, vol. 66, pp. 115409–1–10. <https://doi.org/10.1103/PhysRevB.66.115409>
5. Lee S. I., Howell S. W., Raman A., Reifengerger R. Nonlinear dynamic perspectives on dynamic force microscopy. *Ultramicroscopy*, 2003, vol. 97, no. 1/4, 25 p. [https://doi.org/10.1016/s0304-3991\(03\)00043-3](https://doi.org/10.1016/s0304-3991(03)00043-3)
6. Hu Sh., Raman A. Analytical formulas and scaling laws for peak interaction forces in dynamic atomic force microscopy. *Applied Physics Letters*, 2007, vol. 91, pp. 123106–1–3. <https://doi.org/10.1063/1.2783226>
7. Kiracofe D., Melcher J., Raman A. Gaining insight into the physics of dynamic atomic force microscopy in complex environments using the VEDA simulator. *Review of Scientific Instruments*, 2012, vol. 83, no. 1, pp. 013702–1–17. <https://doi.org/10.1063/1.3669638>
8. Guzman H. V., Garcia P. D., Garcia R. Dynamic force microscopy simulator (dForce): A tool for planning and understanding tapping and bimodal AFM experiments. *Beilstein Journal of Nanotechnology*, 2015, vol. 6, pp. 369–379. <https://doi.org/10.3762/bjnano.6.36>
9. Wagner T. Steady-state and transient behavior in dynamic atomic force microscopy. *Journal of Applied Physics*, 2019, vol. 125, no. 4, pp. 044301–1–13. <https://doi.org/10.1063/1.5078954>
10. Bahrami M. R. Dynamic analysis of atomic force microscope in tapping mode. *Vibroengineering Procedia*, 2020, vol. 32, 7 p. <https://doi.org/10.21595/vp.2020.21488>
11. Chandrashekar A., Belardinelli P., Lenci S., Stauffer U., Alijani F. Mode coupling in dynamic atomic force microscopy. *Physical Review Applied*, 2021, vol. 15, no. 2, pp. 024013–1–11. <https://doi.org/10.1103/PhysRevApplied.15.024013>
12. Melcher J., Hu Sh., Raman A. Invited Article: VEDA: A web-based virtual environment for dynamic atomic force microscopy. *Review of Scientific Instruments*, 2008, vol. 79, no. 6, pp. 061301–1–11. <https://doi.org/10.1063/1.2938864>
13. Thorén P.-A., Borgani R., Forchheimer D., Dobryden I., Claesson P. M., Kassa H. G., Leclère Ph. [et al.]. Modeling and measuring viscoelasticity with dynamic atomic force microscopy. *Physical Review Applied*, 2018, vol. 10, no. 2, pp. 024017–1–13. <https://doi.org/10.1103/PhysRevApplied.10.024017>
14. Keyvani A., Tamer M. S., Wingerden J.-W. van, Goosen J. F. L., Keulen F. van. A comprehensive model for transient behavior of tapping mode atomic force microscope. *Nonlinear Dynamics*, 2019, vol. 97, pp. 1601–1617. <https://doi.org/10.1007/s11071-019-05079-2>

15. Farokh Payam A., Morelli A., Lemoine P. Multiparametric analytical quantification of materials at nanoscale in tapping force microscopy. *Applied Surface Science*, 2021, vol. 536, pp. 147698-1–15. <https://doi.org/10.1016/j.apsusc.2020.147698>
16. Johnson K. L. *Contact Mechanics*. Cambridge University Press, 1987. 452 p.
17. Abetkovskaia S. O., Chizhik S. A. Dynamic force spectroscopy of «soft» materials. *Тепло- и массоперенос – 2007: сборник научных трудов* [Heat and Mass Transfer – 2007: Scientific Papers]. Minsk, A. V. Luikov Institute of Heat and Mass Transfer of the National Academy of Sciences of Belarus, 2007, pp. 323–330 (in Russian).
18. Garcia R., Gómez C. J., Martinez N. F., Patil S., Dietz C., Magerle R. Identification of nanoscale dissipation processes by dynamic atomic force microscopy. *Physical Review Letters*, 2006, vol. 97, no. 1, pp. 016103-1–4. <https://doi.org/10.1103/PhysRevLett.97.016103>